PAPER

Energy levels of a spin–orbit-coupled Bose–Einstein condensate in a double-well potential

IOP Publishing | Astro Ltd Laser Physics

Laser Phys. **25** (2015) 025501 (7pp) doi:10.1088/1054-660X/25/2/025501

Energy levels of a spin–orbit-coupled Bose–Einstein condensate in a double-well potential

Wen-Yuan Wang[1,2], Hui Cao[2], Shi-Liang Zhu[3], Jie Liu[1,2,4] and Li-Bin Fu[2,4]

[1] School of Physics, Beijing Institute of Technology, Beijing 100081, People's Republic of China
[2] National Laboratory of Science and Technology on Computational Physics, Institute of Applied Physics and Computational Mathematics, Beijing 100088, People's Republic of China
[3] National Laboratory of Solid State Microstructures and School of Physics, Nanjing University, Nanjing 210093, People's Republic of China
[4] Center for Applied Physics and Technology, Peking University, Beijing 100084, People's Republic of China

E-mail: hcao.physics@gmail.com and lbfu@iapcm.ac.cn

Received 5 November 2014, revised 15 November 2014
Accepted for publication 17 November 2014
Published 24 December 2014

Abstract

We investigate the energy levels of a spin–orbit-coupled Bose–Einstein condensate in a double-well potential under the mean-field approximation. We find that the energy levels of the system can be significantly influenced by the atomic interactions. Without atomic interaction, four energy levels change linearly with the tunneling amplitude, the Raman coupling, and the spin–orbit coupling. However, whenever atomic interaction is considered, three more energy levels will appear, which have a nonlinear dependence on those parameters above. These three energy levels are multi-degenerate and related to the macro-symmetry of the system.

Keywords: energy levels, spin–orbit-coupled BEC, double-well potential, macro-symmetry

(Some figures may appear in colour only in the online journal)

1. Introduction

The experimental realization of artificial gauge fields in neutral atom systems [1–8] has attracted a great deal of attention in the ultracold physics community. So far, both abelian and non-abelian gauge fields have been realized for quantum gases using the two-photon Raman process [1, 9–11]. The realized non-abelian gauge field leads to a particular spin–orbit (SO) coupling, which can be regarded as an equal-weight combination of Rashba and Dresselhaus SO coupling [12]. In such systems, the strength of the coupling can be optically tuned, which is also a useful tool for ultracold fermions [13, 14]. These achievements have stimulated theoretical efforts in understanding the SO effects and have brought much excitement both theoretically and experimentally in this many-body system, such as superstripes and the excitation spectrum [15], quantum tricriticality and phase transitions [16], supercurrent and dynamical instability [17], Majorana fermions [18], the Zitterbewegung effect [19–21], which is characterized by high-frequency oscillations (trembling motion) for Dirac electrons, and the Fulde–Ferrell–Larkin–Ovchinnikov phase of Fermi gases [22–25].

Interesting quantum effects have been found when ultracold atoms are loaded in a double-well trapping potential, such as atomic Josephson effects [26–29], and macroscopic quantum self-trapping [30–33]. Analysis of the energy level of such a system provides an insight into these phenomena [34, 35]. Besides the conventional single species Bose–Einstein condensates (BECs), the dynamics of two-species BECs and spinor BECs in a double-well potential have also been studied [36, 37]. More recently, the dynamics of spin–orbit-coupled (SOC) BECs in a double-well potential has been investigated [38–42]. However, to our knowledge, the energy levels of the SOC ultracold atoms in the double-well

potential have not yet been studied, which may provide an insight into their dynamics.

The aim of this paper is to investigate the energy levels of an SOC BEC in a double-well trapping potential in the mean-field framework. In the absence of atomic interaction, the energy levels change linearly with the tunneling amplitude, the Raman coupling, and the SO coupling strengths. However, when the atomic interaction takes place, the energy levels are changed completely. Three more energy levels appear even for an arbitrarily weak atomic interaction, which change nonlinearly with respect to the Raman coupling strength. The analytical expressions of the energy levels are obtained, and are consistent with the numerical results. Moreover, we find that these three new energy levels are multi-degenerate and related to the macro-symmetry of the system.

The paper is organized as follows. We introduce in section 2 the model describing an SOC BEC in a double-well potential. In section 3, we analyze the energy levels of the system, and discuss the effects of the tunneling amplitude, the Raman coupling, the SO coupling, and the atomic interaction on the energy levels. In section 4, we show in detail the degeneracy of the energy levels and relate them to the macro-symmetry. A brief conclusion is finally given in section 5.

2. Model

Spin–orbit coupling in a cold atom system has been successfully demonstrated in dilute gases of ultracold ^{87}Rb atoms at NIST [3], in which the Raman dressing scheme is based on coupling two atomic hyperfine states of $5S_{1/2}$, $|F = 1, m_F = 0\rangle$ and $|F = 1, m_F = -1\rangle$, labeled as spin-up $|\uparrow\rangle$ and spin-down $|\downarrow\rangle$, respectively. The second-quantized Hamiltonian of the Raman dressed BEC confined by a double-well potential $V(x)$ in terms of the creation and annihilation field operators $\hat{\Psi}(x)$ and $\hat{\Psi}^{\dagger}(x)$ is

$$\hat{H} = \int \mathrm{d}x \hat{\Psi}^{\dagger}(x) \left[\frac{\hbar^2 \hat{k}_x^2}{2m} + \hat{V}(r) + \hat{H}_{\mathrm{soc}} + \hat{H}_{\mathrm{int}} \right] \hat{\Psi}(x) \quad (1)$$

with $\hat{\Psi} = \left(\hat{\Psi}_{\uparrow}, \hat{\Psi}_{\downarrow}\right)^T$ being the normalized wave function in the dressed-state representation. $\hat{k}_x$ is the atomic wave vector operator, and m is the atom mass. The SO coupling term is written as

$$\hat{H}_{\mathrm{soc}} = 2\alpha \hat{k}_x \sigma_z + \frac{\Omega}{2}\sigma_x + \frac{\delta}{2}\sigma_z, \quad (2)$$

where Ω is the Raman coupling strength, δ is the detuning of the Raman drive from the level splitting, $\alpha = E_r/k_{\mathrm{L}}$ is the SO coupling strength with $E_r = \hbar^2 k_{\mathrm{L}}^2 / 2m$ being the single-photon recoil energy and k_{L} is the wave number of the Raman laser, and $\sigma_{x(z)}$ is the Pauli matrix. The atom–atom collision interactions are described by

$$\hat{H}_{\mathrm{int}} = \mathrm{diag}\left(\sum_{\sigma=\uparrow,\downarrow} u_{\uparrow\sigma} |\hat{\Psi}_{\sigma}|^2, \sum_{\sigma=\uparrow,\downarrow} u_{\downarrow\sigma} |\hat{\Psi}_{\sigma}|^2 \right), \quad (3)$$

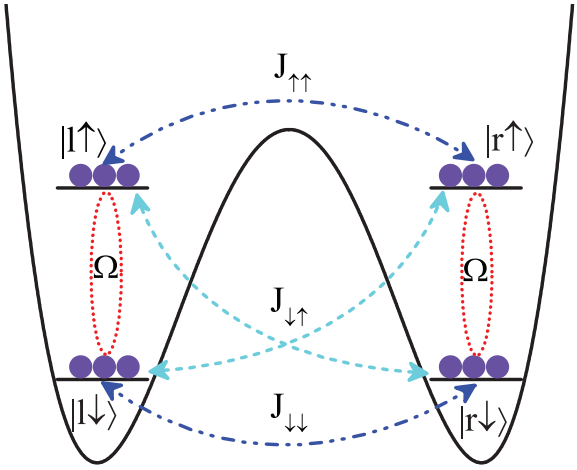

Figure 1. A schematic representation of an SOC BEC in a double-well trap.

where $u_{\sigma\sigma'} = \dfrac{2\hbar^2 a_{\sigma\sigma'}}{ml^2}$ with σ, $\sigma' = \uparrow, \downarrow$ as the interaction strength, $a_{\sigma\sigma'}$ the s-wave scattering length between pseudospin σ and σ', and l the oscillator length associated to a harmonic vertical confinement. For ^{87}Rb atoms, the differences between the spin-dependent nonlinear coefficients are very small and contribute only small modifications to the collective behavior. For the parameters used in the present paper, we have $u_{\uparrow\downarrow} = u_{\downarrow\downarrow} = u_{\uparrow\uparrow}$ [43].

Now let us consider such an SOC BEC in a spin independent symmetric double-well potential, and the system is schematically shown in figure 1. Such a double-well potential can be experimentally realized following the scheme in [32] with the form $V(x) = c(x^2 - d^2)^2$, where the parameters c and d are both tunable. Under the two-mode approximation, the field operator can be written as

$$\hat{\Psi}_{\sigma}(x) = \hat{a}_{l\sigma}\psi_{l\sigma}(x) + \hat{a}_{r\sigma}\psi_{r\sigma}(x), \quad (4)$$

where $\psi_{j\sigma}(x)$ is the ground-state wave function of the j well ($j = l$, r) with pseudo-spin up or down ($\sigma = \uparrow, \downarrow$) and the operator $\hat{a}_{j\sigma}$ $\left(\hat{a}_{j\sigma}^{\dagger}\right)$ is the annihilation (creation) operator for spin σ in the j well. The functions $\psi_{j\sigma}(x)$ satisfy the following orthonormalization conditions: $\int \mathrm{d}x |\psi_{j\sigma}(x)|^2 = 1$ and $\int \mathrm{d}x \psi_{l\sigma}^{*}(x)\psi_{r\sigma}(x) = 0$.

By substituting equation (4) in equation (1), one can rewrite the total Hamiltonian as

$$\begin{aligned} \hat{H} = &\left(\sum_{\sigma\sigma'} J_{\sigma\sigma'} \hat{a}_{l\sigma}^{\dagger} \hat{a}_{r\sigma'} + \frac{\Omega}{2} \sum_j \hat{a}_{j\uparrow}^{\dagger} \hat{a}_{j\downarrow} + \mathrm{h.c.} \right) \\ &+ \frac{\delta}{2} \sum_j \left(\hat{a}_{j\uparrow}^{\dagger} \hat{a}_{j\uparrow} - \hat{a}_{j\downarrow}^{\dagger} \hat{a}_{j\downarrow} \right) + \sum_j \sum_{\sigma\sigma'} \frac{g_{\sigma\sigma'}}{2} \hat{a}_{j\sigma}^{\dagger} \hat{a}_{j\sigma}^{\dagger} \hat{a}_{j\sigma'} \hat{a}_{j\sigma'} \end{aligned} \quad (5)$$

with $g_{\sigma\sigma'} = u_{\sigma\sigma'} N \int \mathrm{d}x |\psi_{j\sigma}|^2 |\psi_{j\sigma'}|^2$. Here $J_{\uparrow\downarrow} = \int \mathrm{d}x \psi_{l\uparrow}^{*}(x) \dfrac{\Omega}{2} \psi_{r\downarrow}(x)$ is the interwell spin-flip tunneling amplitude, i.e. the SO coupling, induced by the Raman coupling, and $J_{\sigma\sigma} = \int \mathrm{d}x \psi_{l\sigma}^{*}(x) \left[\dfrac{\hbar^2}{2m} (k_x^2 \pm 2k_{\mathrm{L}}k_x) \pm \dfrac{\delta}{2} + V(x) \right] \psi_{r\sigma}(x)$ is

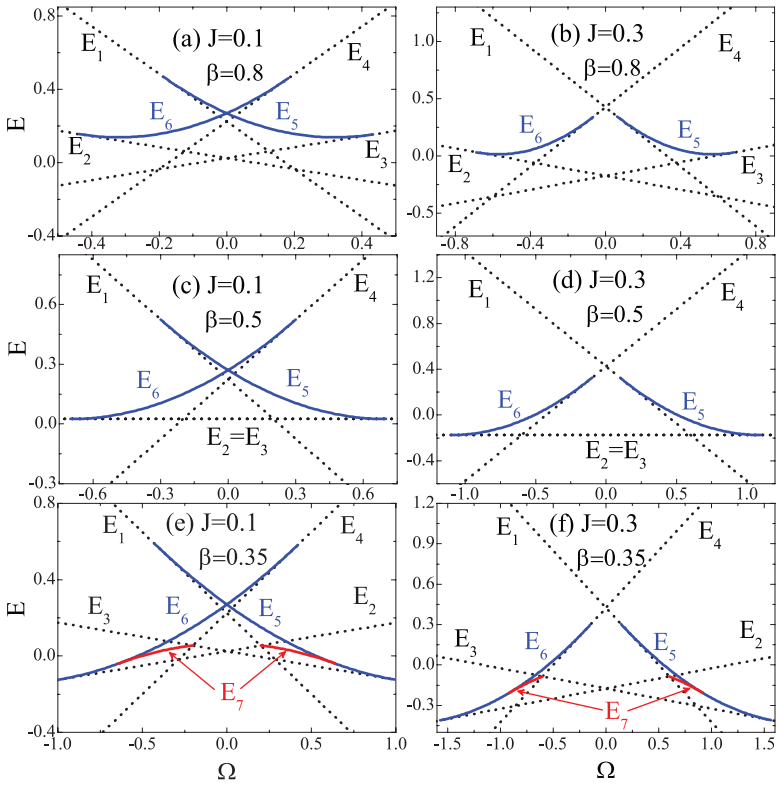

Figure 2. The energy levels versus the Raman coupling strength Ω, where $g = 0.5$. (*a*)–(*b*) for the strong SO coupling strength ($\beta = 0.8$), (*c*)–(*d*) for the intermediate SO coupling strength ($\beta = 0.5$), (*e*)–(*f*) for the relatively weak SO coupling strength ($\beta = 0.35$). (*a*), (*c*), (*e*) $J = 0.1$; (*b*), (*d*), (*f*) $J = 0.3$.

the Josephson tunneling amplitude between the left and right wells with the positive and negative signs corresponding to spin-up and spin-down respectively.

In the Heisenberg picture, one can easily obtain the equations of motion from $\mathrm{i}\dfrac{\mathrm{d}}{\mathrm{d}t}\hat{a}_{j\sigma} = \left[\hat{a}_{j\sigma}, \widehat{H}\right]$ with the Hamiltonian (5). In the mean-field approximation, the operator $\hat{a}_{j\sigma}$ can be replaced by its expectation value $\langle\hat{a}_{j\sigma}\rangle$. For simplicity, we denote this c number with $a_{j\sigma}$. The SOC system is then described by the following equations

$$\mathrm{i}\frac{\mathrm{d}}{\mathrm{d}t}a_{j\sigma} = J_{\sigma\sigma}a_{j'\sigma} + J_{\sigma\sigma'}a_{j'\sigma'} + \frac{\Omega}{2}a_{j\sigma'} + (-1)^p\frac{\delta}{2}a_{j\sigma} + g_{\sigma\sigma}|a_{j\sigma}|^2a_{j\sigma} + g_{\sigma\sigma'}|a_{j\sigma'}|^2a_{j\sigma}\,. \tag{6}$$

Here $j \neq j'$, and $\sigma \neq \sigma'$, and $p = 0, 1$ for $\sigma = \uparrow, \downarrow$ respectively. The number of particles with spin σ is given by $N_{l\sigma} + N_{r\sigma} = |a_{l\sigma}|^2 + |a_{r\sigma}|^2 = N_\sigma$, and the total number of particles $N = N_\uparrow + N_\downarrow$ is conserved.

Since the parameters in the equations of motion (6) are all experimentally tunable [1–3], we take, for simplicity, $J_{\uparrow\uparrow} = J_{\downarrow\downarrow} = J$ and $g_{\sigma\sigma'} = g_{\sigma\sigma} = g$. The SO coupling strength is linearly dependent on the Raman coupling [38], i.e. $J_{\uparrow\downarrow} = \beta\Omega$. Since the Zeeman field δ is independently tunable and should be small, in the following discussions, we take $\delta = 0$.

3. Energy levels of the SOC BEC

The stationary states of the system can be obtained from the following equations

$$\mu a_{j\sigma} = Ja_{j'\sigma} + \beta\Omega a_{j'\sigma'} + \frac{\Omega}{2}a_{j\sigma'} + g_{\sigma\sigma}|a_{j\sigma}|^2a_{j\sigma} + g_{\sigma\sigma'}|a_{j\sigma'}|^2a_{j\sigma} \tag{7}$$

with the probability conservation condition $\Sigma_{j,\sigma}|a_{j\sigma}|^2 = 1$, where μ is the chemical potential, $j \neq j'$, and $\sigma \neq \sigma'$.

When the atomic interaction vanishes, our model reduces to the linear case and the four energy levels can be obtained directly as

$$E_1^0 = J - \beta\Omega - \frac{\Omega}{2}, \tag{8}$$

$$E_2^0 = -J - \beta\Omega + \frac{\Omega}{2}, \tag{9}$$

$$E_3^0 = -J + \beta\Omega - \frac{\Omega}{2}, \tag{10}$$

$$E_4^0 = J + \beta\Omega + \frac{\Omega}{2}\,. \tag{11}$$

These four energy levels are linearly related to the tunneling amplitude $J_{\sigma\sigma}$, the Raman coupling Ω and the SO coupling $\beta\Omega$.

When the atomic interaction is considered, new stationary states emerge for the equation (7). One can intuitively understand that an interaction not only modifies the stationary states of the linear case but can stabilize other states as well and thus create additional stationary states. In the following, we discuss the energy levels in three cases: the

Table 1. The stationary states and their properties.

	$a_{l\uparrow}$	$a_{l\downarrow}$	$a_{r\uparrow}$	$a_{r\downarrow}$	S_{lx}	S_{lz}	S_{rx}	S_{rz}	P
$\|E_1\rangle$	−0.5	0.5	−0.5	0.5	−0.25	0	−0.25	0	1
$\|E_2\rangle$	−0.5	−0.5	0.5	0.5	0.25	0	0.25	0	−1
$\|E_3\rangle$	0.5	−0.5	−0.5	0.5	−0.25	0	−0.25	0	−1
$\|E_4\rangle$	0.5	0.5	0.5	0.5	0.25	0	0.25	0	1
$\|E_5^1\rangle$	ξ_1	$-\xi_1$	ξ_2	$-\xi_2$	χ_2	0	χ_1	0	×
$\|E_5^2\rangle$	ξ_2	$-\xi_2$	ξ_1	$-\xi_1$	χ_1	0	χ_2	0	×
$\|E_6^1\rangle$	ξ_3	ξ_3	$-\xi_4$	$-\xi_4$	χ_3	0	χ_4	0	×
$\|E_6^2\rangle$	ξ_4	ξ_4	$-\xi_3$	$-\xi_3$	χ_4	0	χ_3	0	×
$\|E_7^1\rangle$	ξ_5	ξ_6	$-\xi_7$	$-\xi_8$	χ_5	κ_1	χ_6	$-\kappa_2$	×
$\|E_7^2\rangle$	ξ_6	ξ_5	$-\xi_8$	$-\xi_7$	χ_5	$-\kappa_1$	χ_6	κ_2	×
$\|E_7^3\rangle$	ξ_7	ξ_8	$-\xi_5$	$-\xi_6$	χ_6	$-\kappa_2$	χ_5	κ_1	×
$\|E_7^4\rangle$	ξ_8	ξ_7	$-\xi_6$	$-\xi_5$	χ_6	κ_2	χ_5	$-\kappa_1$	×

strong SO coupling regime ($\beta > 0.5$), the intermediate SO coupling regime ($\beta = 0.5$), and the relatively weak SO coupling regime ($\beta < 0.5$).

First, we consider the energy levels of the system in the strong SO coupling regime, which means that the interwell spin-flip tunneling strength $J_{\sigma\sigma'}$ is stronger than the Raman coupling strength Ω (i.e. $\beta > 0.5$). We plot the mean-field energies as functions of the Raman coupling strength Ω with $g = 0.5$ and $\beta = 0.8$ in figures 2(a) and (b) for $J = 0.1$ and $J = 0.3$ respectively. They show that the four linear energy levels E_{1-4} still exist but their values are shifted by $g/4$. Besides them, two energy levels E_5 and E_6 appear. The tunneling amplitude J does not change the number of levels, but it changes the positions of the new energy levels $E_{5,6}$. As the tunneling amplitude increases, the energy levels E_5 and E_6 move to separate (as shown in figures 2(a) and (b)). When the tunneling amplitude is equal to a half of the interaction strength, the energy levels E_5 and E_6 just separate. For an even stronger tunneling amplitude, the energy levels E_5 and E_6 no longer intersect (as shown in figure 2(b)).

For the interwell SO coupling strength $J_{\sigma\sigma'}$ equal to the Raman coupling strength ($\beta = 0.5$), all the energy levels have a similar distribution with those in the relatively strong SO coupling regime, except that the energy levels E_2 and E_3 are degenerate (figures 2(c) and (d)). The atomic interaction does not change the degeneracy.

We now discuss the energy levels of the system in the relatively weak SO coupling regime. In this regime, the SO coupling strength $J_{\sigma\sigma'}$ is weaker than the Raman coupling strength Ω (i.e. $\beta < 0.5$). We take $\beta = 0.35$ as an example and plot the mean-field energy levels as functions of the Raman coupling strength Ω in figures 2(e) and (f). The major difference between this regime and the above two regimes is the appearance of another energy level E_7, which is the joint action of the tunneling amplitude, SO coupling strength, Raman coupling and atomic interaction.

It is worth noting that the energy levels E_5, E_6 and E_7 just appear under certain conditions. The energy level E_5 appears under the conditions $J - \beta\Omega + g/2 > 0$ and $J - \beta\Omega - g/2 < 0$, the energy level E_6 appears under the conditions $J + \beta\Omega + g/2 > 0$ and $J + \beta\Omega - g/2 < 0$, and the energy level E_7 just appears under the conditions $-g - 4\beta J < \Omega < -2J$, $2J < \Omega < g + 4\beta J$ and $\beta < 0.5$.

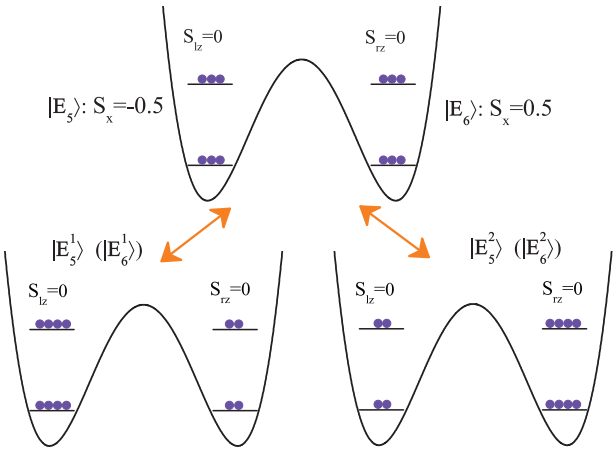

Figure 3. Schematic representation of symmetry breaking and the resulting degenerate states for the energy levels E_5 and E_6.

In the above calculation, we find the interaction only gives rise to a shift $g/4$ for E_{1-4},

$$E_i = E_i^0 + \frac{g}{4} \quad (i = 1, 2, 3, 4)\,. \tag{12}$$

While for the energy levels E_{5-7}, the energy shift induced by the interaction is nonlinear,

$$E_5 = E_1 + \frac{1}{g}\left(J - \beta\Omega - \frac{g}{2}\right)^2, \tag{13}$$

$$= E_3 + \frac{1}{g}\left(J - \beta\Omega + \frac{g}{2}\right)^2, \tag{14}$$

$$E_6 = E_2 + \frac{1}{g}\left(J + \beta\Omega + \frac{g}{2}\right)^2, \tag{15}$$

$$= E_4 + \frac{1}{g}\left(J + \beta\Omega - \frac{g}{2}\right)^2. \tag{16}$$

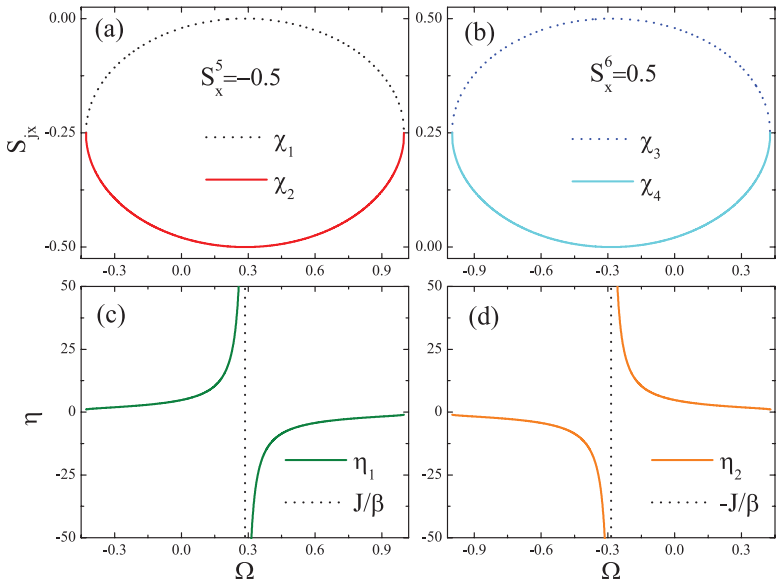

Figure 4. The properties of stationary states for the energy levels E_5 and E_6. (*a*) and (*b*) for S_{jx} of the energy levels E_5 and E_6 respectively. (*c*) and (*d*) for the proportion $\eta = a_{l\sigma}/a_{r\sigma}$ of the two identical spin states between the double wells for E_5 and E_6, where $J = 0.1$, $\beta = 0.35$, and $g = 0.5$.

$$E_7 = E_1 + \frac{1}{g}\left(J - \frac{g}{2}\right)^2 - \frac{1}{g}\left(\frac{\Omega}{2} - \frac{g}{2}\right)^2 + \frac{1}{g}\left(\beta\Omega + \frac{g}{2}\right)^2 - \frac{1}{g}\left(2\beta J + \frac{g}{2}\right)^2, \tag{17}$$

$$= E_2 + \frac{1}{g}\left(J + \frac{g}{2}\right)^2 - \frac{1}{g}\left(\frac{\Omega}{2} + \frac{g}{2}\right)^2 + \frac{1}{g}\left(\beta\Omega + \frac{g}{2}\right)^2 - \frac{1}{g}\left(2\beta J + \frac{g}{2}\right)^2, \tag{18}$$

$$= E_3 + \frac{1}{g}\left(J + \frac{g}{2}\right)^2 - \frac{1}{g}\left(\frac{\Omega}{2} - \frac{g}{2}\right)^2 + \frac{1}{g}\left(\beta\Omega - \frac{g}{2}\right)^2 - \frac{1}{g}\left(2\beta J + \frac{g}{2}\right)^2, \tag{19}$$

$$= E_4 + \frac{1}{g}\left(J - \frac{g}{2}\right)^2 - \frac{1}{g}\left(\frac{\Omega}{2} + \frac{g}{2}\right)^2 + \frac{1}{g}\left(\beta\Omega - \frac{g}{2}\right)^2 - \frac{1}{g}\left(2\beta J + \frac{g}{2}\right)^2. \tag{20}$$

All these results are consistent with the numerical solutions from directly solving the equation (7).

4. Symmetry and degeneracy of the energy levels

To understand more clearly the stationary states and the degeneracy of the above levels, we introduce spin operators $\hat{S}_{jx} = \frac{1}{2}\left(\hat{a}_{j\downarrow}^\dagger \hat{a}_{j\uparrow} + \hat{a}_{j\uparrow}^\dagger \hat{a}_{j\downarrow}\right)$, $\hat{S}_{jy} = \frac{1}{2i}\left(\hat{a}_{j\uparrow}^\dagger \hat{a}_{j\downarrow} - \hat{a}_{j\downarrow}^\dagger \hat{a}_{j\uparrow}\right)$, $\hat{S}_{jz} = \frac{1}{2}\left(\hat{a}_{j\uparrow}^\dagger \hat{a}_{j\uparrow} - \hat{a}_{j\downarrow}^\dagger \hat{a}_{j\downarrow}\right)$, $\hat{S}_x = \hat{S}_{lx} + \hat{S}_{rx}$, and the parity operator $\hat{P} : \left(\hat{a}_{l\uparrow}, \hat{a}_{l\downarrow}\right) \leftrightarrow \left(\hat{a}_{r\uparrow}, \hat{a}_{r\downarrow}\right)$, which interchanges the two wells labeled by l and r. The spin operators defined above reflect the symmetry of the occupation of spin-up and spin-down states in the same well, and the parity reflects the symmetry of the same spin state between the double wells. In the mean-field approximation, we have $\langle\hat{S}_{j,xyz}\rangle \equiv S_{j,xyz}$, $\langle\hat{S}_x\rangle \equiv S_x$ and $\langle\hat{P}\rangle \equiv P$ with $S_{j,\,xyz}$, S_x and P being c numbers. The stationary states and their energy level properties are shown in table 1.

The non-degenerate stationary states $|E_{1-4}\rangle$ of the energy levels E_{1-4} exist at odd or even parity when identical spin states exchange between the left and right wells. Specifically, for $|E_1\rangle$ and $|E_4\rangle$ ($|E_2\rangle$ and $|E_3\rangle$), the parity is even (odd); that is, the exchange of identical spin states between the two wells is symmetric (anti-symmetric). On the other hand, as we can see from table 1, the different spin states in the same well exhibit anti-symmetry for the stationary states $|E_1\rangle$ and $|E_3\rangle$, and symmetry for the stationary states $|E_2\rangle$ and $|E_4\rangle$. For all these stationary states $|E_{1-4}\rangle$, $S_{jz} = 0$, which reflects that the distribution of the particle numbers in the four modes ($l\uparrow$, $l\downarrow$, $r\uparrow$, $r\downarrow$) is always the same.

For the energy levels E_5 and E_6, the parity breaking (shown in table 1) leads to double-degeneracy for both of them. The schematic representations for two degenerate states $|E_5^{1,2}\rangle$ $\left(|E_6^{1,2}\rangle\right)$ of the energy level $E_5(E_6)$ are shown in figure 3. For the $|E_5^{1,2}\rangle$ and $|E_6^{1,2}\rangle$, two identical spin states no longer exhibit symmetry between the double wells. However, the ratio of the probability amplitudes for identical spin states, $\eta = a_{l\sigma}/a_{r\sigma}$, takes on, for the two degenerate states $|E_5^1\rangle$ and $|E_5^2\rangle$ $\left(|E_6^1\rangle$ and $|E_6^2\rangle\right)$, two values η_1 and $1/\eta_1$ (η_2 and $1/\eta_2$) that are reciprocal, respectively. We show in figures 4(*c*) and (*d*) the variation of η with respect to the Raman coupling strength. Also we can easily derive the expectations of the spin operators. For two degenerate states of the energy level E_5, S_{lx} and S_{rx} take on χ_1 and χ_2, or χ_2 and χ_1 respectively. In general, $\chi_{1,2}$ has different values. In figures 4(*a*) and (*b*) we show the

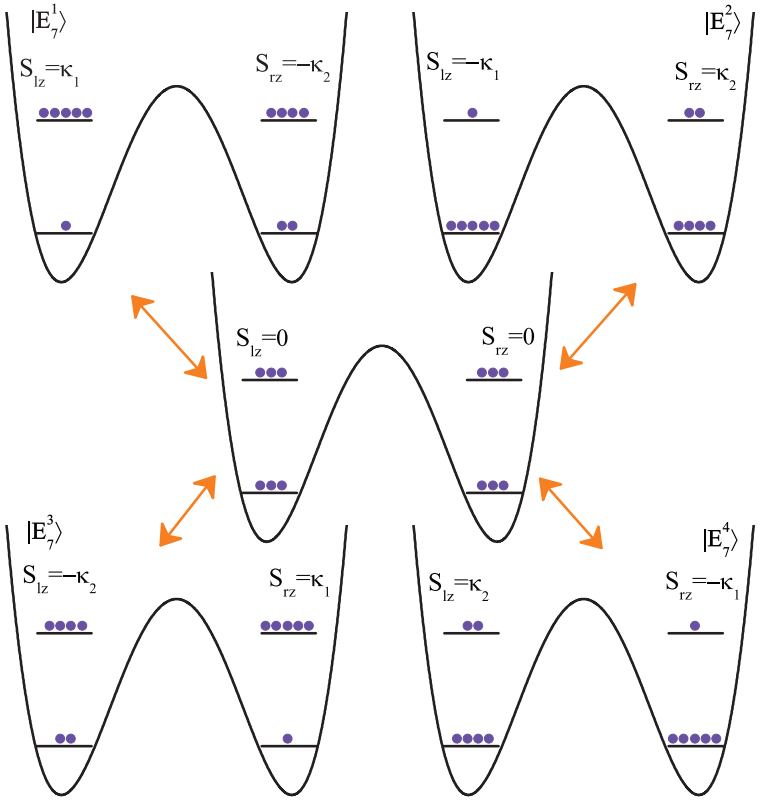

Figure 5. Schematic representation of symmetry breaking and the resulting degenerate states for the energy level E_7.

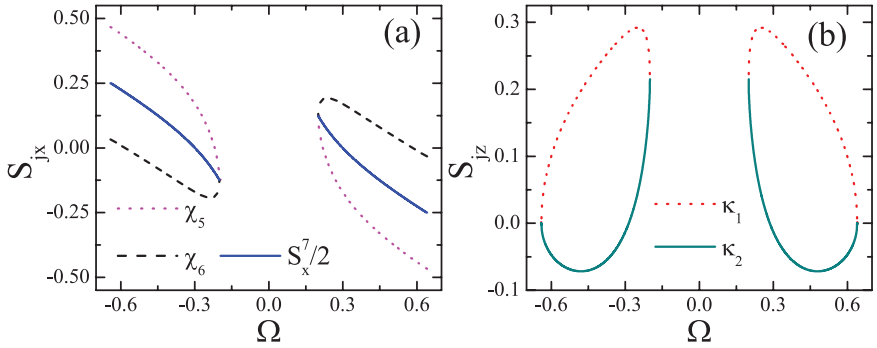

Figure 6. The properties of the stationary states for the energy level E_7. (*a*) and (*b*) for S_{jx} and S_{jz} respectively, where $J = 0.1$, $\beta = 0.35$, $g = 0.5$.

variation of S_{jx} with respect to the Raman coupling strength. Combining the sign of S_{jx} and $S_{jz} = 0$ shows that different spin states in the same well exhibit anti-symmetry for each of the degenerate states $|E_5^1\rangle$ and $|E_5^2\rangle$. The case is similar for the degenerate states of the energy level E_6 except that they exhibit symmetry for each of the degenerate states $|E_6^1\rangle$ and $|E_6^2\rangle$. The values of the total spin S_x do not change with the system parameters; specifically, for $|E_5^{1,2}\rangle$ and $|E_6^{1,2}\rangle$, $S_x^5 = -0.5$ and $S_x^6 = 0.5$, respectively. This difference in the angular momentum can be used to distinguish the energy levels E_5 and E_6 from each other.

For the energy level E_7, the symmetry breaking leads to four degenerate states $|E_7^1\rangle$, $|E_7^2\rangle$, $|E_7^3\rangle$ and $|E_7^4\rangle$ (see the schematic representation in figure 5). For each of these four states, S_{jx} and S_{jz} change with the system parameters. Figures 6(*a*) and (*b*) show the changes of S_{jx} and S_{jz} with the Raman coupling strength respectively. One can see the symmetry breaks for different spin states in the same well, and for identical spin states between two wells.

The energy levels E_{5-7} show macro-symmetry between different stationary states of the same energy level. Although for each state of E_5, the symmetry between the left and right wells is broken, the two stationary states $|E_5^1\rangle$ and $|E_5^2\rangle$ are symmetric with respect to each other under the exchange of the left and right wells, and so are the states $|E_6^1\rangle$ and $|E_6^2\rangle$. The stationary states of the energy level E_7 have rich symmetry properties with respect to each other. Two pairs of stationary states, $|E_7^{1,3}\rangle$ and $|E_7^{2,4}\rangle$, are symmetric under the exchange of the two wells,

respectively, whereas another combination of two pairs of stationary states, $|E_7^{1,2}\rangle$ and $|E_7^{3,4}\rangle$, shows the symmetry under the exchange of spin-up and spin-down.

5. Conclusion

In summary, we have presented a comprehensive analysis of the energy levels for a specific SOC BEC in a double-well trapping potential. The mean-field analysis shows that the energy levels are modified significantly by the atomic interaction: three energy levels emerge as long as the interaction is included. The effects of the tunneling amplitude, the SO coupling, and the Raman coupling on the energy levels are also illustrated. The analytical expressions of the mean-field energies are obtained, which are consistent with the numerical results. We also investigated the degeneracy of the energy levels and the related symmetries of each stationary state. The symmetry breaking induces the multi-degeneracy of the energy levels. Moreover, we investigated the macro-symmetry of the system, i.e. the symmetric properties between the stationary states of the degenerate energy levels. Since the SOC BECs have already been achieved in recent experiments, and the system parameters are highly tunable, we hope our results will stimulate the experiment in this direction.

Acknowledgments

This work is supported by the National Fundamental Research Program of China (Contracts No. 2013CBA01502, No. 2011CB921503, and No. 2013CB834100) and the National Natural Science Foundation of China (Contracts No. 11374040, No. 11274051 and 11125417).

References

[1] Lin Y J, Compton R L, Perry A R, Phillips W D, Porto J V, Spielman I B 2009 *Phys. Rev. Lett.* **102** 130401
Lin Y J, Compton R L, García K J, Porto J V and Spielman I B 2009 *Nature* **462** 628
[2] Lin Y J, Compton R L, García K J, Phillips W D, Porto J V and Spielman I B 2011 *Nat. Phys.* **7** 531
[3] Lin Y J, García K J and Spielman I B 2011 *Nature* **471** 83
[4] Fu Z, Wang P, Chai S, Huang L and Zhang J 2011 *Phys. Rev.* A **84** 043609
[5] Aidelsburger M, Atala M, Nascimbeñe S, Trotzky S, Chen Y A and Bloch I 2011 *Phys. Rev. Lett.* **107** 255301
[6] Struck J, Ölschläger C, Targat R L, Panahi P S, Eckardt A, Lewenstein M, Windpassinger P and Sengstock K 2011 *Science* **333** 996
[7] Zhang J Y *et al* 2012 *Phys. Rev. Lett.* **109** 115301
[8] Williams R A, LeBlanc L J, García K J, Beeler M C, Perry A R, Phillips W D and Spielman I B 2012 *Science* **335** 314
[9] Wang P, Yu Z Q, Fu Z, Miao J, Huang L, Chai S, Zhai H and Zhang J 2012 *Phys. Rev. Lett.* **109** 095301
[10] Cheuk L W, Sommer A T, Hadzibabic Z, Yefsah T, Bakr W S and Zwierlein M W 2012 *Phys. Rev. Lett.* **109** 095302
[11] Zhu S L, Fu H, Wu C J, Zhang S C, Duan L M 2006 *Phys. Rev. Lett.* **97** 240401
Liu X J, Liu X, Kwek L C and Oh C H 2007 *Phys. Rev. Lett.* **98** 026602
[12] Dong L, Jiang L, Hu H and Pu H 2013 *Phys. Rev.* A **87** 043616
[13] Dalibard J, Gerbier F, Juzeliūnas G and Öhberg P 2011 *Rev. Mod. Phys.* **83** 1523
[14] Chapman M and Sa de Melo C A R 2011 *Nature* **471** 41
[15] Li Y, Martone G I, Pitaevskii P L and Stringari S 2013 *Phys. Rev. Lett.* **110** 235302
[16] Li Y, Pitaevskii P L and Stringari S 2012 *Phys. Rev. Lett.* **108** 225301
[17] Ozawa T, Pitaevskii P L and Stringari S 2013 *Phys. Rev.* A **87** 063610
[18] Zhu S L, Shao L B, Wang Z D and Duan L M 2011 *Phys. Rev. Lett.* **106** 100404
[19] Zhang Y C, Song S W, Liu C F and Liu W M 2013 *Phys. Rev.* A **87** 023612
[20] Qu C L, Hamner C, Gong M, Zhang C W and Engels P 2013 *Phys. Rev.* A **88** 021604
[21] Jentschura U D and Noble J H 2013 *Phys. Rev.* A **88** 022121
[22] Iskin M 2013 *Phys. Rev.* A **88** 013631
[23] Wu F, Guo G C, Zhang W and Yi W 2013 *Phys. Rev.* A **88** 043614
[24] Seo K J, Zhang C W and Tewari S 2013 *Phys. Rev.* A **88** 063601
[25] Xu Y, Qu C L, Gong M and Zhang C W 2014 *Phys. Rev.* A **89** 013607
[26] Javanainen J 1986 *Phys. Rev. Lett.* **57** 3164
[27] Milburn G J, Corney J, Wright E M and Walls D F 1997 *Phys. Rev.* A **55** 4318
[28] Smerzi A, Fantoni S, Giovanazzi S, Shenoy S R 1997 *Phys. Rev. Lett.* **79** 4950
Raghavan S, Smerzi A, Fantoni S and Shenoy S R 1999 *Phys. Rev.* A **59** 620
[29] Giovanazzi S, Smerzi A and Fantoni S 2000 *Phys. Rev. Lett.* **84** 4521
[30] Levy S, Lahoud E, Shomroni I and Steinhauer J 2007 *Nature* **449** 579
[31] Albiez M, Gati R, Fölling J, Hunsmann S, Cristiani M and Oberthaler M K 2005 *Phys. Rev. Lett.* **95** 010402
[32] LeBlanc L J, Bardon A B, McKeever J, Extavour M H T, Jervis D, Thywissen J H, Piazza F and Smerzi A 2011 *Phys. Rev. Lett.* **106** 025302
[33] Betz T *et al* 2011 *Phys. Rev. Lett.* **106** 020407
[34] Karkuszewski Z P, Sacha K and Smerzi A 2002 *Eur. Phys. J.* D **21** 251–4
[35] Wu B and Liu J 2006 *Phys. Rev. Lett.* **96** 020405
[36] Tian J, Qiu H B, Wang G F, Chen Y and Fu L B 2013 *Phys. Rev.* E **88** 032906
[37] Satija I I, Balakrishnan R, Naudus P, Heward J, Edwards M and Clark C W 2009 *Phys. Rev.* A **79** 033616
[38] Zhang D W, Fu L B, Wang Z D and Zhu S L 2012 *Phys. Rev.* A **85** 043609
[39] Yu Z F and Xue J K 2014 *Phys. Rev.* A **90** 033618
[40] Struck J, Simonet J and Sengstock K 2014 *Phys. Rev.* A **90** 031601
[41] Garcia-March M A, Mazzarella , Dell'Anna G L, Juliá-Díaz B, Salasnich L and Polls A 2014 *Phys. Rev.* A **89** 063607
[42] Citro R and Naddeo A 2014 arXiv: 1405.5356
[43] Hamner C, Qu C L, Zhang Y P, Chang J J, Gong M, Zhang C W and Engels P 2014 *Nat. Commun.* **5** 4023